



## A Parking Pose and Trajectory Selection Algorithm Based on Artificial Potential Field and Particle Swarm Optimization

Wei Huang<sup>1</sup> , Xiangzhi Wei<sup>2</sup> , Jiaye Zhu<sup>3</sup>  and Kaining Dai<sup>4</sup> 

<sup>1</sup> Shanghai Jiao Tong University, [hweigo@sjtu.edu.cn](mailto:hweigo@sjtu.edu.cn)

<sup>2</sup> Shanghai Jiao Tong University, [antonwei@sjtu.edu.cn](mailto:antonwei@sjtu.edu.cn)

<sup>3</sup> Shanghai Jiao Tong University, [jiayezhu@sjtu.edu.cn](mailto:jiayezhu@sjtu.edu.cn)

<sup>4</sup> Shanghai Jiao Tong University, [836526236@sjtu.edu.cn](mailto:836526236@sjtu.edu.cn)

**Abstract.** Path planning is one of the fundamental issues for automated valet parking system. However, current automatic parking system solutions simply choose the center of the parking bay as target parking pose, which is not the most suitable pose in many situations. Besides, it requires further study to effectively evaluate the parking trajectory; particularly, the path generator might not figure out the suitable trajectory if adjacent vehicle is improperly parked. This paper presents a low-risk parking pose and trajectory selection approach based on the information of the ultrasonic radar and vision. To evaluate the positions of obstacles and parking lines when parking, we design a virtual potential field that can effectively represent the real parking scenario. Thereafter, a Particle Swarm Optimization approach is used to determine the parking pose with the least risk. We use a trajectory configuration to define possible trajectory which connects the initial pose with the final parking pose, and thereafter optimize it by PSO as well to minimize the risk degree, and finally smooth the path by spline interpolation. The experimental results show that our method can adaptively adjust the parking poses in different parking scenarios, which leads to a feasible and smooth parking trajectory.

**Keywords:** Automated Valet Parking, Collision Detection, Artificial Potential Field, Particle Swarm Optimization, Spline Interpolation

**DOI:** <https://doi.org/10.14733/cadconfP.2022.988-999>

### 1 INTRODUCTION

Automated Valet Parking (AVP) system is one of the hottest research topics in advanced driver-assistance systems. Path planning is a crucial part of the AVP system. It's responsible to calculate a reasonable collision-free parking path from the initial parking state to the desired goal position to help drivers finish the final parking process. Compared with driving on an urban road or highway, parking performs at a relatively slow speed but in a much narrower and more compact environment, which makes it difficult to find a feasible and suitable parking path.

## 1.1 State of the Art

Several methods have been proposed to generate a feasible trajectory for the automated parking system. The most representative one is Reeds and Shepp [13], which first proposed a path planning method for car-like robots by connecting the initial position and target position with line segments and circular arcs to avoid obstacles. Wang et al. also presented a double circular trajectory generator for perpendicular parking based on geometrical information [19]. The drawback of these approaches is that the curvature is not continuous at the joints of the segments, meaning that the ego vehicle needs to stop at the joints which will induce faster wearing of the tires. Therefore, more and more researchers start to focus on continuous-curvature path generators. Fraichard et al. adopted Reeds and Shepp's work and present a clothoid planning scheme where clothoid arcs are included to combine with line segments and arcs of circles [14]. Vorobieva et al. proposed a parallel parking method that generates smooth clothoid curves to help park the vehicle into tiny parking spots in one or more maneuvers [18]. Besides clothoid curve, B-splines was used to smooth the trajectory in [6] and Bezier curve was used in [8]. Some other methods using the geometric method can be found in [16, 17, 20].

Other than conventional geometric methods mentioned above, several randomized sampling-based planning algorithms have been proposed for the planning task of the vehicles [2, 22]. Jeong et al. proposed a planning algorithm based on Rapidly-exploring Random Tree (RRT) [3]. However, due to the compact environment of parking scenarios, RRT algorithm might find it hard to obtain a feasible path into the parking slot.

The above methods merely discuss how to derive a feasible parking trajectory but have not discussed how to determine the path most suitable to the present parking scenario. Neural network scheme has been studied to implement in the parking process in [9]. But it highly relies on human expert's knowledge and thus is hard to apply to the real-world parking scenario if training data is limited [16]. Li et al. formulated a dynamic model based on kinematic principle and environment information and introduced an interior-point simultaneous approach to optimize the model to derive the parking path [7]. Jing et al. proposed a path planning algorithm based on sequential quadratic programming for parallel parking [4]. Some more work done with optimization can be found in [10, 21]. However, these optimization methods either minimized the length of the parking trajectory, which seems trivial since the lengths differ slightly in compact parking area, or tuned the curve to avoid collisions, which can only guarantee the path is feasible but not the most suitable.

## 1.2 Contribution and Content of This Paper

Many advanced driver-assistance systems using ultrasonic radar and camera are now commercially available for several manufacturers (e.g., Tesla and NIO). In this paper, we present a novel parking path planning algorithm for this kind of multi-sensor detection scheme. The proposed method is able to determine the optimal parking pose for parking the car in one maneuver from an arbitrary starting pose. The contribution of this paper are summarized as follows:

- We fuse the ultrasonic radar and vision information with a modified artificial potential field algorithm. By assigning different weights for obstacles and parking lane markers, the algorithm can thoroughly represent the real parking scenario and treat different types of objects with different risks. This allows our path planning algorithm to effectively avoid obstacle collisions and park ego vehicle into the target parking slot.
- Currently, most of the parking path planning algorithms choose the final parking pose by selecting the position at the middle of the parking slot or parking the car between two adjacent vehicles. However, in some parking scenarios, the former strategy may cause the ego vehicle to park too close to obstacles, while the latter strategy cannot handle the situation when there is no adjacent vehicle. To mitigate these problems, we propose a general parking pose selection algorithm that can determine the optimal parking pose for

different parking scenarios, including the case when some adjacent vehicle is not parked properly.

- To generate a feasible trajectory from the initial parking state to the final parking pose. We present an innovative path planning algorithm that combines conventional geometric methods and an optimization-based method that utilizes PSO to tune the parking poses and trajectory control parameters and figure out the optimal parking path with the least risky degree, which makes our algorithm robust and effective.

The paper is organized as follows: Section 2 introduces the methodology. Section 3 presents the experimental result conducted in MATLAB platform. Finally, conclusions and some discussions are given in section 4.

## 2 METHODOLOGY

Our approach mainly contains three steps: (1) a virtual potential field is constructed to help assess the risk degree within the parking scenario; (2) the final parking pose with the least risk is determined; (3) a smooth and effective path is computed to connect the initial pose with the final parking pose, and the path can be used to guide the vehicle’s parking maneuver.

### 2.1 Artificial Potential Field Construction and Cost Evaluation

Considering the high price of lidar, nowadays most vehicles use cameras or ultrasonic radar for advanced driver-assistance systems. The camera can obtain the lane line information on the road using lane-line detection algorithm, and the ultrasonic radar can quickly detect physical obstacles such as other vehicles and fences [15]. In this paper, an artificial potential field method is used in our approach to fuse the information of the ultrasonic radar and vision camera such that the circumstances around the vehicle can be better evaluated.

Artificial potential field is a commonly used path planning algorithm introduced by Khatib [5]. However, considering that parking normally happens in narrow areas, directly using conventional artificial potential field method often fails to find a feasible solution [12]. Also, the algorithm cannot guarantee that the motion of the vehicle satisfies kinematic constraints. Therefore, in our approach, an improved artificial potential field method is developed to help evaluate the safety of the surrounding environment, and the parking path is defined geometrically and optimized in the configuration space.

Let  $W$  denote the 2-D Euclidean parking plane. To distinguish the two different types of obstacles in the neighborhood of the parking space detected by ultrasonic radars and cameras, the following notation is used in this paper [1]. Physical obstacles detected by ultrasonic radar are represented as the compact sets of points  $OU_i, i = 1, 2, \dots, n$  in  $W$ . And the parking lines detected by the camera are represented as  $OC_i, i = 1, 2, \dots, m$ . As shown in Equation (2.1), the potential energy  $U$  at point  $x$  is computed by summing up the effects of all the neighboring obstacles. For a specific obstacle point  $OU_i$  or  $OC_i$ , the potential energy at point  $x$  is computed by Equation (2.2).

$$U(x) = \sum_{j \in OU} U_j(x) + \sum_{j \in OC} U_j(x) \tag{2.1}$$

$$U_j(x) = \begin{cases} U_{j \max} & d_j(x) = 0 \\ 0.5 * \eta_j * \left( \frac{1}{d_j(x)} - \frac{1}{Q_j} \right)^2 & 0 < d_j(x) \leq Q_j \\ 0, & d_j(x) > Q_j \end{cases} \tag{2.2}$$

Where,

$$U_{OU \max} \gg U_{OC \max}, \eta_{OU} \gg \eta_{OC}, Q_{OU} \gg Q_{OC} \tag{2.3}$$

where  $d_j(x)$  is the distance from point  $x$  to the obstacle  $j$ ,  $\eta_j$  is the potential repulsive constant,  $Q_j$  is the range of the influence of obstacle  $j$ . During the auto-parking process, the ego vehicle first needs to ensure that it can avoid physical obstacles and maintain a safe margin with nearby vehicles, and park the entire car into the parking spot according to the parking line markers information. Therefore, for obstacles  $OU$  detected by ultrasonic radars,  $U_{j\max}$ ,  $\eta_j$ , and  $Q_j$  are assigned with large values to ensure that the vehicle keeps a safe distance from obstacles. For the parking lines  $OC$  detected by the cameras, these parameters are assigned with relatively small values. Their relationship is described in Equation (2.3). In this way, our algorithm can fuse sensor information and evaluate different obstacle's effects on the car separately.

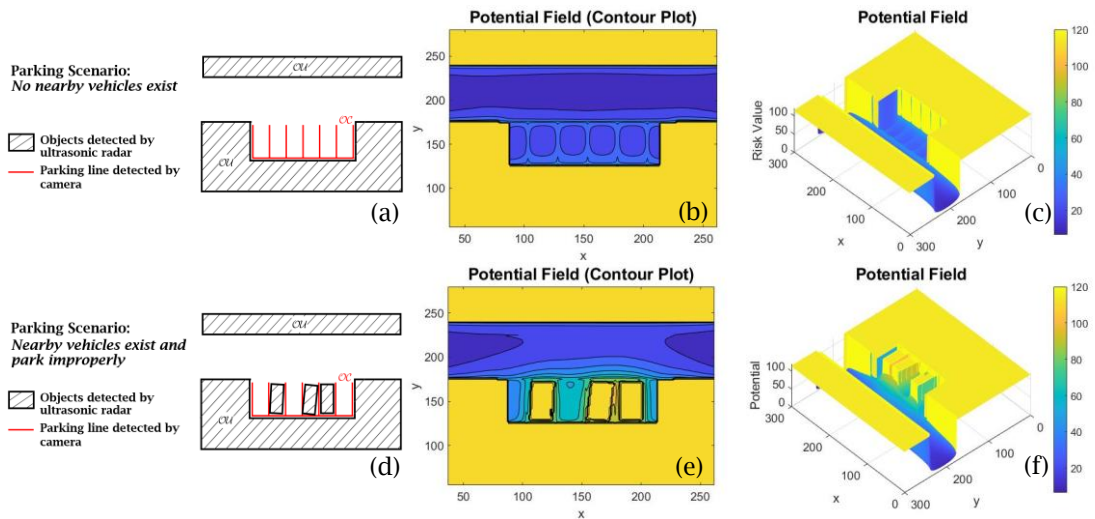


**Figure 1:** The first row shows the parking scenario without nearby vehicles: (a) Parking lot map, (b) Potential filed (contour plot), (c) Potential filed. The second row shows the parking scenario when nearby vehicles are tilted, (d) Parking lot map, (e) Potential filed (contour plot), (f) Potential filed.

Figure 1 shows two common parking scenarios and the corresponding potential fields. Figure 1(a)(d) is the initial parking environment. The hatched regions denote obstacles detected by ultrasonic radars and the red lines denote parking line markers detected by cameras. Figure 1(c)(f) show the corresponding potential fields, and Figure 1(b)(e) are the contour plot views. The higher the potential energy (the yellow part in the figure), the more likely the vehicle collides with obstacles or crosses the lane lines.

## 2.2 Optimal Parking Pose Computation

To describe the final parking pose of the vehicle, three control parameters are used: vehicle center's coordinate  $[x, y]^T$ , and the vehicle's heading angle  $\theta$  relative to x-axis. Hence, the pose configuration can be represented as  $q = [x, y, \theta]^T$ . All possible final parking poses form the configuration space  $C$ , which is a Euclidean group of  $SE(2) = \mathbb{R}^2 \times SO(2)$ . Let  $A(q)$  be a subset of  $C$  referring to the points covered by the body of the vehicle at configuration  $q$ . After constructing the potential field, the risk degree for a given vehicle pose  $q$  can be measured by sampling the vehicle coverage space  $A(q)$  and computing its average potential energy. Therefore, the problem of

selecting the optimal parking pose can be transformed into the problem of finding the vehicle pose that minimizes the average potential energy.

$$\begin{aligned} \min_{q \in C} f_{pose}(q) &= \frac{1}{n} \sum_{p \in A(q)} U(p) \\ \text{s.t. } x_{\min} &\leq x \leq x_{\max} \\ y_{\min} &\leq y \leq y_{\max} \\ \theta_{\min} &\leq \theta \leq \theta_{\max} \end{aligned} \quad (2.4)$$

Where  $n$  is the population of the sample and  $p$  refers to the sample point in the vehicle coverage area  $A(q)$ . Figure 2 demonstrates the pose sampling process where the background is the potential field generated previously. We first determine the area covered by ego vehicle's current pose and sample discrete points within it (indicated as the black dots in Figure 2). The average potential energy of all sampling points is used to represent the risk of current pose and used as the objective function in Equation (2.4).

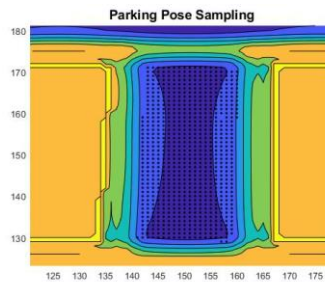


**Figure 2:** The parking pose sampling demonstration.

We then use PSO to solve the above optimization problem and determine the optimal pose. Within the configuration space  $C$ , particles are first initialized with an arbitrary pose configuration  $q = [x, y, \theta]^T$ . The velocity attribute  $v_i^t$  determines the particle's position in the next iteration. The iteration rule is shown as follows:

$$q_i^{t+1} = q_i^t + v_i^{t+1} \quad (2.5)$$

$$v_i^{t+1} = \omega v_i^t + c_1 r_1 (Q_i^t - q_i^t) + c_2 r_2 (G^t - q_i^t) \quad (2.6)$$

Where,  $q_i^t$  is the position of the particle  $i$  at the  $t$  th iteration, and  $v_i^t$  is the velocity of the particle  $i$  at the  $t$  th iteration. The first term in the velocity expression reflects the inertia of the particle. The second and third terms are the velocity components pointing to the optimal position of the individual and the optimal position of the swarm, respectively. The hyperparameters  $\omega$ ,  $c_1$ , and  $c_2$  have a great influence on the final result. In our experiments, we gradually converge  $\omega$  from 1.0 to 0.4. In this case, a strong  $\omega$  avoid the searching falls into local best solution at the beginning while a weaker  $\omega$  could speed up convergence once particles are close to the global best solution. For the individual and global acceleration coefficients, we use  $c_1 = 1.5$  and  $c_2 = 1.5$ , which is found to determine the optimal solution efficiently, usually in less than 30 iterations. Within limit iteration steps, the global best cost becomes stable and its corresponding particle's position  $q_{best} = [x, y, \theta]^T$  can be taken as the optimal parking pose.

### 2.3 Kinematic Model and Trajectory Definition

Since parking is a relatively slow movement with small acceleration and jerk, several assumptions can be made: (1) the car is a rigid body; (2) the car is restricted to move in a plane; (3) there is no sliding at the contact point of wheels and the ground. Therefore, the kinematic model of the vehicle can be simplified as the Ackermann steering model, also known as the bicycle model. This kinematic model is illustrated in Figure 3(a).

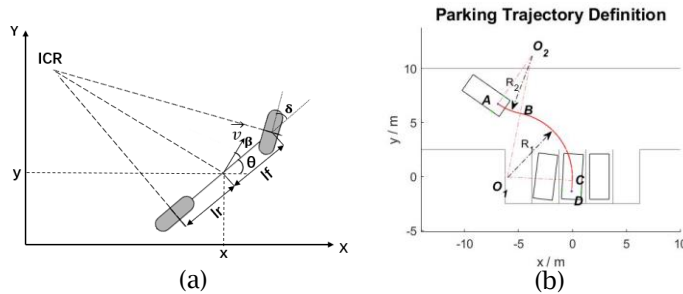


**Figure 3:** (a)Ackermann steering model, (b) Parking trajectory definition.

In the reference coordinate system,  $[x, y, \theta]^T$  illustrate the vehicle’s pose. The ego vehicle rotates around ICP, instantaneous center of rotation, with radius  $R$ .  $\vec{v}$  represents the vehicle’s current velocity and  $\beta$  represents the heading angle.  $\delta$  refers to the steering angle and  $l_r, l_f$  is the distance from the center of vehicle to the front/rear axle. According to the non-holonomic constraints shown in Figure 3(a), the ego vehicle kinematics can be expressed as

$$\begin{aligned} \frac{dx(t)}{dt} &= v \cdot \cos(\beta(t) + \varphi(t)) \\ \frac{dy(t)}{dt} &= v \cdot \sin(\beta(t) + \varphi(t)) \\ \frac{d\varphi(t)}{dt} &= \frac{v}{l_r} \cdot \sin(\beta(t)) \end{aligned} \tag{2.7}$$

Where,

$$\varphi(t) = \arctan\left(\frac{l_r}{l_f + l_r} \cdot \tan(\delta(t))\right) \tag{2.8}$$

As mentioned in Section 1.1, several parking path generators have been designed using circular arcs and line segments and then the path is further smoothed. This is a straightforward and efficient approach by studying a driver’s behavior. In this paper, we follow these previous works and define the parking trajectory template as shown in Figure 3(b). Two arcs are used to guide the vehicle from the starting point A to point B, and then point B to point C, with the turning radius of  $R_2$  and  $R_1$ , respectively. Then, a line segment with distance  $d$  guides the vehicle to reverse itself to the final parking position. It is worth mentioning that in the conventional geometrical-base methods, these trajectory control parameters, e.g.  $R_1, R_2$ , and  $d$ , are derived according to the parking environment’s geometric information, e.g. the corners of the parking slot. However, these methods are not robust and cannot guarantee to obtain a suitable parking trajectory. In the next section, we present an optimization approach to fine-tune these parameters and to figure out the optimal parking path with the minimum risk degree.

### 2.4 Optimal Parking Path Computation

Let  $t$  denote a parking trajectory mentioned in Section 2.3, which can be expressed as  $t = [R_1, d]^T$ . All the possible parking trajectories span a 2-D configuration space and can be represented as  $T = \{t = [R_1, d]^T \mid R_1 \geq R_{\min}, R_2 \geq R_{\min}, 0 \leq d \leq d_{\max}\}$ . Here,  $R_{\min}$  is the minimum turning radius according to the Ackermann steering model. For a specific trajectory  $t$ , we sample several poses with a constant step along the path for each segment. When sampling, more sample poses are selected in circular arcs segment, since the car turning process is more likely to accidentally collide with adjacent obstacles. We then use these poses' average covered potential energy as a measure of the risk degree of the trajectory. The optimal trajectory selection problem can thus be transformed into an optimization problem as follow.

$$\begin{aligned} \min_{t \in T} \quad & f_{\text{trajectory}}(t) = \frac{1}{n} \sum_{q \in t} f_{\text{pose}}(q) \\ \text{s.t.} \quad & R_{\min} \leq R_1 \\ & R_{\min} \leq R_2 \\ & 0 \leq d \leq d_{\max} \end{aligned} \tag{2.9}$$

Where,

$$R_2 = \frac{|AO_1|^2 - R_1^2}{2|AO_1| \cos \angle O_2AO_1 + 2R_1} \tag{2.10}$$

Next, PSO is also implemented to search for the parking trajectory  $t$  with the minimum potential energy in  $T$ . In this case, we search for the best trajectory in a two-dimensional space where the particle's position configuration is  $q = [R_1, d]^T$  since  $R_2$  can be derived geometrically once  $R_1, d$  are known according to Equation (2.10). Similar to pose computation, the iteration stops as swarms' global best cost no longer drops.

Since the path generated so far is a composition of circular arcs and line segments, it's discontinuous on the tangent points. This means that the ego vehicle will either needs to be steered or stopped suddenly along the path, which should be avoided. Different smooth curves have been studied to use for creating a continuous-curvature path [11, 16]. Here, we solve this problem by sampling the trajectory to obtain discrete points along the path the same way as measuring the trajectory's risk degree mentioned above. We then use a cubic spline curve to interpolate these points. The property of cubic spline guarantee that the reshaped curve's second derivative is continuous and thus can avoid the above issues. Figure 4 is the curvature comparison before and after path smoothing process. From the figure, we can see that before smoothing (black line), the curvature is discontinuous as it changes abruptly at the points where segments connect. After interpolation, curvature continuity can be achieved (red line), which makes the generated path satisfy kinematic constraint and is able to avoid sudden steering during the parking process.

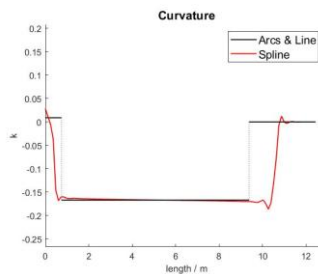


Figure 4: Curvature comparison.

### 3 EXPERIMENTS AND DISCUSSION

The proposed algorithm has been evaluated in MATLAB platform using a virtual parking lot map and random initial parking pose. Section 3.1 demonstrates the optimal parking pose computed under different parking circumstances. Once the final parking pose is determined, the path generator algorithm is tested with different initial poses in Section 3.2. Table 1 presents some specification parameters used in the experiments. In Figure 5-7, the center of the target parking spot is set to be the origin and is perpendicular to x-axis.

Parameters	Notation	Value
Vehicle length	$L_v$	4.2 (m)
Vehicle width	$W_v$	1.7 (m)
Wheelbase	$l_r + l_f$	2.7 (m)
Maximum steering angle	$\delta_{max}$	0.47 (rad)
Parking plot length	$L_p$	5.0 (m)
Parking plot width	$W_p$	2.5 (m)

**Table 1:** Specifications of the vehicle and parking plot.

#### 3.1 Optimal Parking Pose Determination

To evaluate the effectiveness of the proposed algorithm, we tested this pose optimization approach in several parking scenarios frequently encountered in daily life. Figure 5 shows three common cases in the underground garage, one ideal parking scenario, and two less perfect parking scenarios. Refer to Figure 5(a) and (d), case 1 shows the scenario when no adjacent vehicles exist, and the parking process is only guided by parking lane markers. Refer to Figure 5(b) and (e), case 2 is the case when two vehicles are already parked on both sides, but too close to the right parking lane. Refer to Figure 5(c) and (f), case 3 is when the nearby vehicles' heading is not perpendicular to the parking spot. Figure 5(a-c) show the optimal pose's sampling condition in the potential field map. Figure 5(d-e) demonstrate the final parking condition.

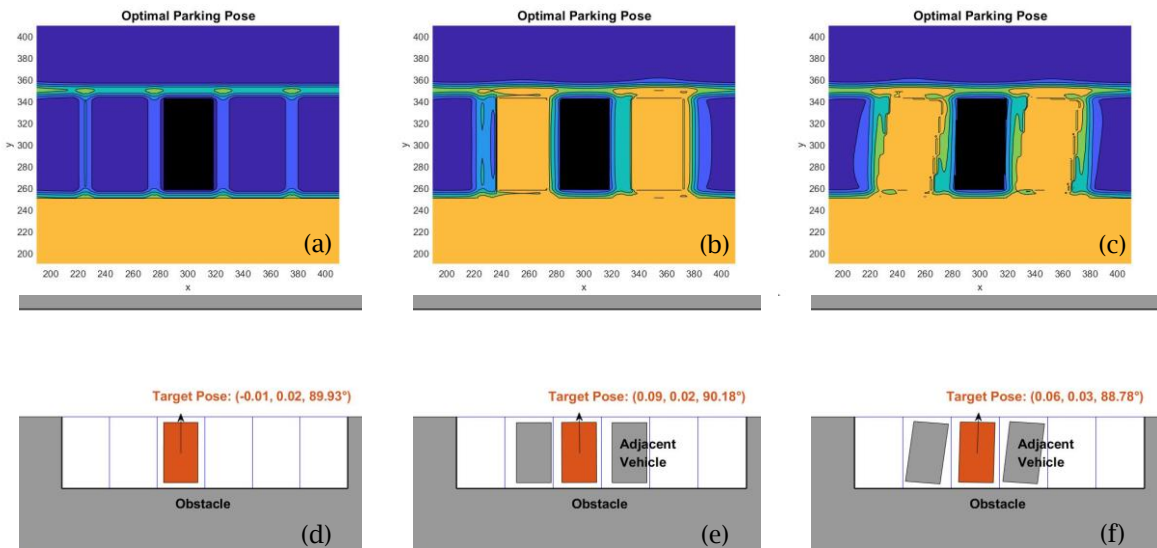


**Figure 5:** Optimal parking poses our approach determined in three cases.

The result shows that our approach is effective no matter whether the parking lane markers or the nearby obstacles exist or not. Thus, it is robust and general for different parking scenarios. Moreover, case 2 and case 3 show that our approach is capable to adjust the final parking pose to guarantee a safe margin between ego vehicle and adjacent vehicles. Even when the adjacent vehicles are too close to the target parking spot (Figure 5(e)) or rotated (Figure 5(f)), the final parking pose is adaptively adjusted to ensure that the driver and the passengers can get out of the car easily, and to avoid collisions when driving out of the parking spot.

Parking Scenario	Parking Pose	x/m	y/m	$\theta/^\circ$	Average Potential Energy
Case 1	Center of parking spot	0.0	0.0	90.0	21.867
	Center of nearby vehicles	0.0	0.0	90.0	21.867
	<b>Our method</b>	-0.01	0.02	89.93	21.924
Case 2	Center of parking spot	0.0	0.0	90.0	23.048
	Center of nearby vehicles	0.2	0.0	90.0	22.828
	<b>Our method</b>	<b>0.09</b>	<b>0.02</b>	<b>90.18</b>	<b>22.250</b>
Case 3	Center of parking spot	0.0	0.0	90.0	20.573
	Center of nearby vehicles	0.0	0.0	86.0	21.066
	<b>Our method</b>	<b>0.06</b>	<b>0.03</b>	<b>88.78</b>	<b>20.356</b>

**Table 1:** Comparison of the pose result of our method with two common default poses.

As shown in Table 1, we also compare the final parking pose selected by our approach with two common default parking poses, center of parking spot (widely used in vision-based scheme) and center of nearby vehicles (widely used in ultrasonic-based scheme). From the table, we can see that when no adjacent vehicles exist, our pose selection approach chooses to park the car at the center of the parking slot and set it perpendicular with the parking bay, which is the ideal pose. As for the case when adjacent vehicles are improperly parked, our approach can significantly reduce the average potential energy, also regarded as risky degree, by adjusting the position or heading angle to better fit in the scenario.

### 3.2 Determination of the Optimal Parking Pose

We tested the parking path generator with different initial positions and random parking scenarios.

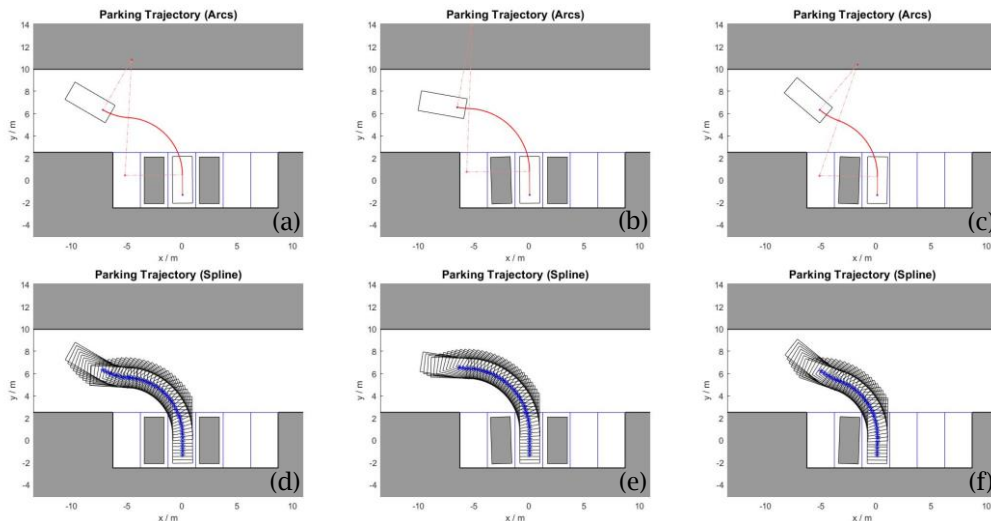


**Figure 6:** Optimal parking trajectories determined in three cases with our approach.

Figure 6 demonstrates the path our approach obtains in three different scenarios. The above figures (Figure 6(a-c)) are the template trajectories composed by line segment and circular arcs and optimized by PSO. The below figures (Figure 6(d-f)) are the trajectories after smoothing and the demonstration of the entire parking process. The result shows that our approach is capable to deal with arbitrary initial poses and different parking scenarios even when the adjacent car is not parked ideally. With our path generator, a feasible and suitable path can be derived to guide the vehicle to drive into the parking spot and park at desired parking pose. We find that the selected path with the least average risk tends to straighten the pose before the entire car enters the parking spot and then uses a long-distance reverse to finish the parking process, which is similar to human drivers' behavior.

We compared our path generator with a widely used approach [4]. The comparison result is shown in Figure 7. Both approaches generate feasible parking paths. A major difference is that the conventional method derives a feasible parking path by computing the possible turning radius and generates the path with Bezier curve, while our approach further evaluates each possible path and determines the one with the least risk degree. Besides, from the local perspectives, shown in Figure 7(b), we can see that our approach selects the final parking pose with a little rotation to better fit in this particular parking scenario. Moreover, since the parking lane markers are given with a small risky influence when constructing virtual potential field in our approach, the generated path adjusts the vehicle's pose earlier than the conventional method and does not even cross any side of the parking lane during the parking process. The results indicate that the proposed approach can guide the vehicle to park into the target parking spot effectively and the performance is ideal even when some adjacent vehicles are not parked properly.

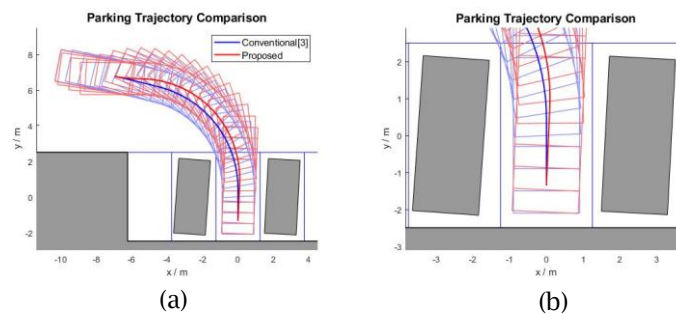


**Figure 7:** Trajectory comparison between our method and conventional method. (a) Overall view, (b) Local perspective view.

#### 4 CONCLUSION

In this paper, we presented an efficient parking path planning algorithm for the multi-sensor detection scheme. To efficiently fuse the information of ultrasonic radar and vision and represent the real parking environment, we developed a virtual potential field to help assess the risk degree of different parking poses and trajectories. In order to derive optimal parking pose, we transformed the pose selecting problem into an optimization objective and solved it using Particle Swarm Optimization to determine the final pose with the least risk. A template parking trajectory was defined to connect the initial pose with the final parking pose, which can be controlled by path configuration. Thereafter, the configuration was optimized by PSO as well to minimize the risk degree, and finally, the trajectory was smoothed by spline interpolation.

The performance of the proposed algorithm has been evaluated via a set of MATLAB simulations. The experimental results showed that our approach can adaptively adjust parking pose to fit different parking scenarios. It is capable of changing the car's position or rotating the heading angle to keep a safe margin with nearby obstacles, and ensuring the entire car is inside

the parking spot. Our path generator is robust to deal with different initial car positions and parking scenarios. Meanwhile, the curvature of the path is continuous after smoothing. We also found that the optimized trajectory is quite similar to an experienced driver's behavior.

For future work, we plan to apply the algorithm to other parking cases, e.g. parallel parking lots and echelon parking lots. In addition, a parallel computing scheme can be integrated into our approach to speed up the construction of the potential field that takes much computation time (which is now  $\sim 1$  sec running via MATLAB on Inter(R) i7-10750H).

Wei Huang, <https://orcid.org/0000-0003-1177-9059>

Xiangzhi Wei, <https://orcid.org/0000-0002-4541-0017>

Jiaye Zhu, <https://orcid.org/0000-0003-4686-4448>

Kaining Dai, <https://orcid.org/0000-0002-6230-6641>

## REFERENCES

- [1] Barraquand, J.; Latombe, J.-C.: Robot motion planning: A distributed representation approach, *The International Journal of Robotics Research*, 10(6), 1991, 628-649. <https://doi.org/10.1177/027836499101000604>
- [2] Bruce, J.; Veloso, M. M.: Real-time randomized path planning for robot navigation, *Robot Soccer World Cup*, 2002, 288-295. [https://doi.org/10.1007/978-3-540-45135-8\\_23](https://doi.org/10.1007/978-3-540-45135-8_23)
- [3] Jeong, Y.; Kim, S.; Jo, B. R.; Shin, H.; Yi, K.: Sampling Based Vehicle Motion Planning for Autonomous Valet Parking with Moving Obstacles, *International Journal of Automotive Engineering*, 9(4), 2018, 215-222. [https://doi.org/10.20485/jsaeijae.9.4\\_215](https://doi.org/10.20485/jsaeijae.9.4_215)
- [4] Jing, W.; Feng, D.; Zhang, P.; Zhang, S.; Lin, S.; Tang, B.: A multi-objective optimization-based path planning method for parallel parking of autonomous vehicle via nonlinear programming, 2018 15th International Conference on Control, Automation, Robotics and Vision (ICARCV), 2018, 1665-1670. <https://doi.org/10.1109/ICARCV.2018.8581195>
- [5] Khatib, O.: Real-time obstacle avoidance for manipulators and mobile robots, *Autonomous robot vehicles*, 1986, 396-404. [https://doi.org/10.1007/978-1-4613-8997-2\\_29](https://doi.org/10.1007/978-1-4613-8997-2_29)
- [6] Komoriya, K.; Tanie, K.: Trajectory design and control of a wheel-type mobile robot using B-spline curve, *Proceedings. IEEE/RSJ International Workshop on Intelligent Robots and Systems' (IROS'89) The Autonomous Mobile Robots and Its Applications*, 1989, 398-405.
- [7] Li, B.; Shao, Z.: A unified motion planning method for parking an autonomous vehicle in the presence of irregularly placed obstacles, *Knowledge-Based Systems*, 86, 2015, 11-20. <https://doi.org/10.1016/j.knosys.2015.04.016>
- [8] Liang, Z.; Zheng, G.; Li, J.: Automatic parking path optimization based on bezier curve fitting, 2012 IEEE International Conference on Automation and Logistics, 2012, 583-587. <https://doi.org/10.1109/ICAL.2012.6308145>
- [9] Liu, W.; Li, Z.; Li, L.; Wang, F.-Y.: Parking like a human: A direct trajectory planning solution, *IEEE Transactions on Intelligent Transportation Systems*, 18(12), 2017, 3388-3397. <https://doi.org/10.1109/TITS.2017.2687047>
- [10] Moon, J.; Bae, I.; Kim, S.: Real-time near-optimal path and maneuver planning in automatic parking using a simultaneous dynamic optimization approach, 2017 IEEE Intelligent Vehicles Symposium (IV), 2017, 193-196. <https://doi.org/10.1109/IVS.2017.7995719>
- [11] Muller, B.; Deutscher, J.; Grodde, S.: Continuous Curvature Trajectory Design and Feedforward Control for Parking a Car, *IEEE Transactions on Control Systems Technology*, 15(3), 2007, 541-553. <https://doi.org/10.1109/TCST.2006.890289>
- [12] Oetiker, M. B.; Baker, G. P.; Guzzella, L.: A navigation-field-based semi-autonomous nonholonomic vehicle-parking assistant, *IEEE Transactions on Vehicular Technology*, 58(3), 2008, 1106-1118. <https://doi.org/10.1109/TVT.2008.928643>
- [13] Reeds, J.; Shepp, L.: Optimal paths for a car that goes both forwards and backwards, *Pacific journal of mathematics*, 145(2), 1990, 367-393. <https://doi.org/10.2140/pjm.1990.145.367>

- [14] Schwesinger, U.; Bürki, M.; Timpner, J.; Rottmann, S.; Wolf, L.; Paz, L. M.; Grimmer, H.; Posner, I.; Newman, P.; Häne, C.; Heng, L.; Lee, G. H.; Sattler, T.; Pollefeys, M.; Allodi, M.; Valenti, F.; Mimura, K.; Goebelsmann, B.; Derendarz, W.; Mühlfellner, P.; Wonneberger, S.; Waldmann, R.; Grysczyk, S.; Last, C.; Brüning, S.; Horstmann, S.; Bartholomäus, M.; Brummer, C.; Stellmacher, M.; Pucks, F.; Nicklas, M.; Siegwart, R.: Automated valet parking and charging for e-mobility, 2016 IEEE Intelligent Vehicles Symposium (IV), 2016, 157-164. <https://doi.org/10.1109/IVS.2016.7535380>
- [15] Siegwart, R.; Nourbakhsh, I. R.; Scaramuzza, D.: Introduction to autonomous mobile robots, MIT press, 2011,
- [16] Song, Y.; Liao, C.: Analysis and review of state-of-the-art automatic parking assist system, 2016 IEEE International Conference on Vehicular Electronics and Safety (ICVES), 2016, 1-6. <https://doi.org/10.1109/ICVES.2016.7548171>
- [17] Vorobieva, H.; Minoiu-Enache, N.; Glaser, S.; Mammar, S.: Geometric continuous-curvature path planning for automatic parallel parking, 2013 10th IEEE International Conference On Networking, Sensing And Control (ICNSC), 2013, 418-423. <https://doi.org/10.1109/ICNSC.2013.6548775>
- [18] Vorobieva, H.; Glaser, S.; Minoiu-Enache, N.; Mammar, S.: Automatic Parallel Parking in Tiny Spots: Path Planning and Control, IEEE Transactions on Intelligent Transportation Systems, 16(1), 2015, 396-410. <https://doi.org/10.1109/TITS.2014.2335054>
- [19] Wang, C.; Zhang, H.; Yang, M.; Wang, X.; Ye, L.; Guo, C.: Automatic parking based on a bird's eye view vision system, Advances in Mechanical Engineering, 6, 2014, 847406. <https://doi.org/10.1155/2014/847406>
- [20] Wang, D.; Liang, H.; Mei, T.; Zhu, H.: Research on self-parking path planning algorithms, Proceedings of 2011 IEEE International Conference on Vehicular Electronics and Safety, 2011, 258-262. <https://doi.org/10.1109/ICVES.2011.5983825>
- [21] Zhang, X.; Liniger, A.; Sakai, A.; Borrelli, F.: Autonomous parking using optimization-based collision avoidance, 2018 IEEE Conference on Decision and Control (CDC), 2018, 4327-4332. <https://doi.org/10.1109/CDC.2018.8619433>
- [22] Zheng, K.; Liu, S.: RRT based Path Planning for Autonomous Parking of Vehicle, 2018 IEEE 7th Data Driven Control and Learning Systems Conference (DDCLS), 2018. <https://doi.org/10.1109/DDCLS.2018.8515940>